Ecological Indicators 88 (2018) 351–360

Contents lists available at ScienceDirect

Ecological Indicators

journal homepage: www.elsevier.com/locate/ecolind

The dynamics of sand-stabilization services in Inner Mongolia, China from 1981 to 2010 and its relationship with climate change and human activities

Dajing Li[a], Duanyang Xu[a,*], Ziyu Wang[b], Xiaogang You[c], Xiaoyu Zhang[a], Alin Song[d]

[a] Institute of Geographic Sciences and Natural Resources Research, Chinese Academy of Sciences, Beijing 100101, China
[b] Beijing Forestry University, Beijing 100083, China
[c] Liaoning Technical University, Fuxin 123000, China
[d] Institute of Agricultural Resources and Regional Planning, Chinese Academy of Agricultural Sciences, Beijing 100081, China

ARTICLE INFO

Keywords:
Sand-stabilization service
Climate change
Human activities
Quantitative identification
Inner Mongolia
RWEQ

ABSTRACT

Sand-stabilization, the most important ecological service provided by desert and desertified lands, can alleviate severe wind erosion of soil and is induced by both climate change and human activities. However, with a lack of related data, few studies have focused on the spatial differences in driving factors of sand-stabilization services at a large scale. The present study, based on climatic and socioeconomic data, employed Inner Mongolia as a study area and assessed different climatic and human factors affecting changes of the sand-stabilization services from 1981 to 2010. The results showed that the sand-stabilization service of Inner Mongolia has changed significantly over the past 30 years over an area of 563,584 km^2, and the spatial distribution of the regions affected exhibited considerable heterogeneity. With respect to regions experiencing a significant increase of sand-stabilization service, climate change, human activities, and the coupled effect of the two accounted for 68.49%, 61.25%, and 60.72%, respectively, of the total area experiencing a significant increase in area. Temperature and afforestation projects were the most important drivers of change in these areas. With respect to regions with a significant decrease of sand-stabilization service, climate change, human activities, and the coupled effect of the two accounted for 51.87%, 68.35%, and 42.64%, respectively, of the total area experiencing a significant decrease in area, which was mainly attributed to the increase of livestock stocking rates and crop area.

1. Introduction

Natural ecosystems provide numerous services and goods that support the health and survival of humans, including provisioning, regulating, cultural, and support services (Costanza et al., 1997; Daily, 1997; MA, 2005; TEEB, 2010). As one of the most important ecosystems on earth, deserts and desertified lands occupy 3.37×10^7 km^2 (UNEP, 2006), and provide some critical services including sand-stabilization, soil conservation, maintenance of biodiversity, regulation of water resources, landscape-scale recreation, and so on (Richardson, 2005; Kroeger and Manalo, 2007). The ecological services provided by desert and desertified lands not only support about 500 million people in earth's arid and semi-arid regions, but also have a great impact on the sustainability of global socioeconomic development (UNEP, 2006).

Sand-stabilization is one of the most important ecological services provided by desert and desertified lands, which occurs through a lessening of wind speed, stabilization of soil, and reducing wind erosion (Becker et al., 2015). Sand-stabilization service also has close relationship with sandstorms, and when less sand-stabilization service is provided by desert and desertified lands a higher risk of sandstorms will be created, which might jeopardize human safety and cause losses for agricultural-industrial activities (Chan et al., 2006; Steltzer et al., 2009; Borrelli et al., 2014; Cao et al., 2016). The great value of this sand-stabilization service has caused an ever-increasing number of countries pool efforts to restore vegetation in arid and semi-arid regions with the goal of improving the welfare of local residents. For example, a previous study has shown that the economic value of sand-stabilization increased by $\$5.27 \times 10^6$ in Yuyang, China during the period of 1988–2003 under the large tree-planting program (Mo et al., 2006).

Gaining a better understanding and quantitative measuring the dynamics of sand-stabilization services and their relationship to climate change and human activities in a way that supports integrated policy-making will be a core part of the long-term solutions needed to control desertification (Feng et al., 2015; Galati et al., 2016; Schirpke et al., 2017; Taylor et al., 2017). In recent decades, numerous studies have been conducted to assess the sand-stabilization services provided by desert and desertified lands based on the estimation of wind erosion, and have analyzed the forces driving sand-stabilization at different

* Corresponding author.
E-mail address: xudy@igsnrr.ac.cn (D. Xu).

https://doi.org/10.1016/j.ecolind.2018.01.018
Received 21 October 2017; Received in revised form 28 December 2017; Accepted 10 January 2018
1470-160X/ © 2018 Elsevier Ltd. All rights reserved.

scales (de Oro et al., 2016; Iturri et al., 2016). In these studies, the Revised Wind Erosion Equation (RWEQ) model of United States Department of Agriculture (USDA) has been used to estimate the amount of soil transported by wind (Fryrear et al., 1998; Van Pelt et al., 2004; Fryrear et al., 2000; Jiang et al., 2016b; Fu et al., 2017). For instance, Gong et al. (2014a) applied a RWEQ model to reveal the effects of grassland change on sand-stabilization services since the 1990s in Xilingol League, Inner Mongolia, China. Shen et al. (2016) quantitatively analyzed the temporal and spatial patterns of sand-stabilization services and their driving forces between 2000 and 2010 while using an RWEQ model in Hunshandake, China.

In fact, the mechanism used to create a sand-stabilization service is relatively complicated, because it is affected by climate, soil, vegetation, and other factors. With respect to climatic factors, higher temperatures or lower precipitation can result in drier soils and limit crop production, and eventually exacerbate wind erosion (McFarlane et al., 2012; Sharratt et al., 2015; Kerns et al., 2017; Marzen et al., 2017). As an exogenous force, wind also has a significant influence on wind erosion (Kidron et al., 2017; Schmidt et al., 2017). In addition, the presence of vegetation can increase the surface roughness of an area and minimize the effects of erosion caused by air flow on the ground surface, so vegetation can provide the benefit reducing the amount of wind erosion (Wolfe and Nickling, 1993; Cerdan et al., 2010; Liu et al., 2014). Also, scholars have gained a more consistent understanding of how increasing vegetation coverage can provide an effective measure to improve the sand-stabilization service (Pierre et al., 2015; Keesstra et al., 2018). However, human activities can change the land use and vegetation coverage of the underlying surface, and thus have an effect on soil erosion and sand-stabilization services (Serpa et al., 2015; Jiang et al., 2016c). Research has shown that land reclamation, firewood cutting, excessive use of water resources, and other unsustainable economic activities have seriously damaged the vegetation in some areas, creating the main cause of an anthropogenic acceleration of wind erosion (He et al., 2005; Foley et al., 2005; Nelson et al., 2009; Hostert et al., 2011). Some studies had tried to investigate the mechanism involved in the formation of wind erosion by considering both natural and human factors (Arnaud et al., 2016; Latocha et al., 2016); however, it was still difficult to assess the contribution of each factor owing to the complexity of the interaction of different factors. Meanwhile, most related research has focused on the meso-small scale, and little attention has been paid to the spatial differences of driving factors at a large scale due to the lack of related data. In particular, the influence of human activities on wind erosion has not been deeply analyzed, which makes it very difficult to successfully explain the mechanism involved in the formation of sand-stabilization services.

Inner Mongolia is a representative wind erosion zone in northern China. The maintenance and promotion of sand-stabilization services in this region are playing a critical role in guaranteeing the ecological security of North China. Although a great deal of ecological engineering and restoration has been carried out in recent years, extensive human activities such as mining and rapid urbanization have had a great impact on the underlying surface (Vu et al., 2014). These factors coupled with climate change have generated significant changes in the sand-stabilization services of Inner Mongolia. The goals of this research are (1) to identify the dynamics of sand-stabilization services in Inner Mongolia from 1981 to 2010, and (2) to analyze the driving mechanism of climate change and human activities in sand-stabilization service at county scale. The related results are hoped to provide support for policy-makers and land managers involved in ecological compensation and desertification control in arid areas.

2. Materials and methods

2.1. Study area

Inner Mongolia Autonomous Region lies between 37°24′N–53°23′N and 97°12′E–126°04′E in Northern China, and includes a total of 88 counties or banners (hereinafter referred to as counties; Fig. 1 and Table 1). The study area covered approximately 1.18×10^6 km^2, or 12.3% of the country's total area. The temperate zone continental monsoon climate has an average temperature of 0–8 °C and an annual total precipitation or 50–450 mm that progressively decreased from east to west. The region receives an average annual of 2850 h of sunshine and stands at an average elevation of 1000 m. The soils are mostly brown desert, chestnut, and sandy soils. Gales occur on 10–40 days annually, mainly in spring, and 5–20 days with sandstorms. Influenced by climatic factors (such as sandstorms, temperature, precipitation, etc.) and unsustainable human activities (such as grassland reclamation, abandonment of cultivated land, etc.), wind erosion and land degradation are serious problems in this region.

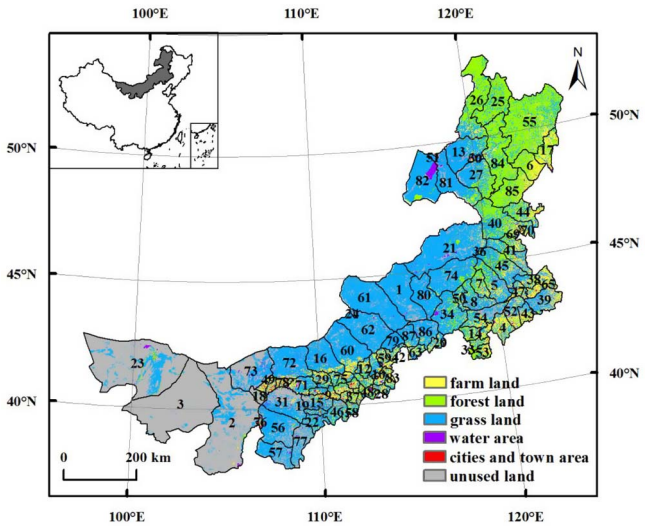

Fig. 1. The location of study area. (The banners and counties represented by each number are listed in Table 1).

2.2. Data collection and processing

The meteorological (including temperature, precipitation, sunshine duration, average wind speed, etc.), snow cover, and soil data used in this study were derived from the Cold and Arid Regions Sciences Data Center. Specifically, meteorological data were acquired from the China Meteorological Forcing Dataset having a time resolution of 3 h, a spatial resolution of 0.1 degrees, and a time range of 1979–2010. The snow cover data were obtained from the Long-term Snow Depth Dataset of China having a time resolution of 1 day, a spatial resolution of 0.25 degrees, and a time range of 1979–2010. Soil particle and organic matter contents were derived from the China Soil Characteristics Dataset having a spatial resolution of 1 km. The Normalized Difference Vegetation Index (NDVI) used in this study was the Global Inventory Modeling and Mapping Studies NDVI3g dataset, with these data obtained from National Aeronautics and Space Administration. The time resolution of this dataset was half of a month with a spatial resolution of 8 km and the time range of 1981–2010. This dataset has been preprocessed by geometric correction and graphic enhancement to ensure data quality. The social-economic data which included urbanization rate, crop area, livestock, and afforestation data at county level were derived from Inner Mongolia's and China's annual forestry statistical yearbooks. In order to facilitate spatial analysis and comparison, all data used in this study were resampled to a grid data with an 8 km resolution. In addition, considering the effects of driving factors was relatively uniform and stable in any one county, the influence of climate change and human activities was analyzed by using the mean values at the county level.

Table 1
The name of the banner/county in Fig. 1.

Num	Name	Num	Name	Num	Name	Num	Name
1	Abaga	23	Ejina	45	Jarud	67	Tumd L
2	Alxa L	24	Erenhot	46	Jungar	68	Tumd R
3	Alxa R	25	Ergun L	47	Kailu	69	Tuquan
4	Aohan	26	Ergun R	48	Liangcheng	70	Ulanhot
5	Ar Horqin	27	Ewenki	49	Linhe	71	Urad F
6	Arun	28	Fengzhen	50	Linxi	72	Urad M
7	Bairin L	29	Guyang	51	Manchuria	73	Urad B
8	Bairin R	30	Hailar	52	Naiman	74	Ujimqin W
9	Baotou	31	Hanggin	53	Ningcheng	75	Wuchuan
10	Chahar RB	32	Hanggin B	54	Ongniud	76	Wuhai
11	Chahar RF	33	Harqin	55	Oroqen	77	Wushen
12	Chahar RM	34	Hexigten	56	Otog	78	Wuyuan
13	Chenbarhu	35	Hohhot	57	Otog F	79	Xianghuang
14	Chifeng	36	Holingola	58	Qingshuihe	80	Xilinhot
15	Dalad	37	Horinger	59	Shangdu	81	Xin Barag L
16	Darhan	38	Horqin LM	60	Siziwang	82	Xin Barag R
17	Daur	39	Horqin LB	61	Sonid L	83	Xinghe
18	Dengkou	40	Horqin RF	62	Sonid R	84	Yakeshi
19	Dongsheng	41	Horqin RM	63	Taibus	85	Zhalantun
20	Duolun	42	Huade	64	Togtoh	86	Zhenglan
21	Ujimqin E	43	Hure	65	Tongliao	87	Zhengxiangbai
22	Ejin Horo	44	Jalaid	66	Tsining	88	Zhuozi

where, L is Left; R is Right; F is Front; B is Back; M is Middle; E is East; W is West.

2.3. Methods

2.3.1. Assessment of sand-stabilization services

In this study, the soil retention rate (hereinafter referred to as *F*) was selected as the indicator used to assess sand-stabilization services; *F* was the ratio of the amount of soil retention (SL_{sv}) to the amount of potential soil erosion under bare soil conditions (SL_s), which could eliminate the influence of climate factors and further analyze the role of ecosystem sand-stabilization. In addition, the RWEQ model was used to estimate the amount of wind erosion occurring over a specific period of time (Gong et al., 2014b; Mendez and Buschiazzo, 2015; Pi et al., 2017). This model fully considered the effects of weather, soils, crops, and tillage roughness, which make the RWEQ model suitable for the assessment of wind erosion in Inner Mongolia. The basic equations are as follows:

$$Q_{\max} = 109.8(WF \times EF \times SCF \times K' \times COG) \quad (1)$$

$$Q_x = Q_{\max}\left[1 - e^{\left(\frac{x}{s}\right)^2}\right] \quad (2)$$

$$s = 150.71(WF \times EF \times SCF \times K' \times COG)^{-0.3711} \quad (3)$$

$$SL_s v = SL_s - SL_v \quad (4)$$

$$F = \frac{SL_s v}{SL_s} \times 100 \quad (5)$$

where Q_{max} is maximum transport (kg/m); Q_x is mass transport at downwind distance x (kg/m); s is the critical field length (m); x is distance from the upwind edge of a field (m); *EF* is the erodible soil fraction; *WF, SCF, K′, COG* are weather, soil, crust soil roughness, and vegetation factor, respectively; SL_{sv} is soil retention; SL_s is soil erosion under bare soil conditions; SL_v is soil erosion under the conditions of the ground cover vegetation; *F* is the soil retention rate.

(1) Weather factor (*WF*)

The WF is mainly determined by wind speed, soil moisture, snow cover, and other factors. It was computed using Formula (6).

$$WF = \frac{\sum_{i=1}^{N} U_2(U_2 - U_t)^2 \times N_d \rho}{N \times g} \times SW \times SD \quad (6)$$

where, U_2 is wind speed at a height of 2 m (m/s); U_t is threshold wind speed at 2 m (assumed wind speed of 5 m/s); N is number of wind speed observations (usually 500); N_d is number of days (usually 15); ρ is air density (kg/m^3); g is acceleration due to gravity (m/s^2); *SW* is soil wetness; *SD* is the snow cover factor.

(2) Soil erodible fraction (*EF*)

The erodible fraction is that fraction of the upper 25 mm of soil that is smaller than 0.84 mm in diameter as determined by a standard compact rotary sieve (Chepil, 1962), which can reflect the influence of soil erosion under a certain soil physico-chemical properties. The present study used the following formula:

$$EF = \frac{29.09 + 0.31Sa + 0.17Si + \frac{0.33Sa}{Cl} - 2.59OM - 0.95CaCO_3}{100} \quad (7)$$

where *Sa* is sand content (5.5%–93.6%); *Si* is silt content (0.5%–69.5%); *Sa/Cl* is the sand to clay ratio (1.2%–53.0%); *OM* is organic matter content (0.32%–4.74%); $CaCO_3$ is calcium carbonate content (0–25.2%). The data given in parenthesis above represent the range of values. $CaCO_3$ was calculated by 0 in this study.

(3) Soil crust factor (*SCF*)

When raindrops impact the soil surface, they break down soil clods and a soil crust may be formed (Zobeck, 1991). Soil crust formation can be calculated by Formula (8):

$$SCF = \frac{1}{1 + 0.0066(Cl)^2 + 0.021(OM)^2} \quad (8)$$

where *Cl* and *OM* have the same meaning as in Formula (7).

(4) Soil roughness factor (K′)

The *K′* can reflect the effect of surface roughness on wind erosion caused by topography. According to previous studies (Gong et al., 2014b), the *K′* of sandy land and grassland are 0.96 and 0.69,

respectively.

(5) Vegetation factor (*COG*)

The *COG* is used to quantify the effects of wind erosion under different types of vegetation cover, and can be calculated with the follows equations:

$$COG = SLR_f \times SLR_s \times SLR_c \quad (9)$$

$$SLR_f = e^{-0.0438(SC)} \quad (10)$$

$$SLR_s = e^{-0.0344(SA^{0.6413})} \quad (11)$$

$$SLR_c = e^{-5.614(CC^{0.7366})} \quad (12)$$

where SLR_f, SLR_s and SLR_c are the soil loss ratio coefficients for flat cover, plant silhouettes, and growing crop canopy, respectively. *SC* is the percent of soil coverage with flat residues, which was estimated by the photos (Gong et al., 2014b); *SA* is silhouette area, which computed by multiplying the number of standing stalks in 1 m^2 times average diameter (cm) times stalk height (cm); *CC* is the fraction of soil surface covered with crop canopy, which was calculated by NDVI values.

2.3.2. Trend analysis of the soil retention rate

In the present study, a linear trend equation and the least squares method were used to analyze the trend of variations in *F* from 1981 to 2010. In addition, a t-test ($p < 0.05$) was used to identify areas where *F* changed significantly and can be described as follows:

$$b_1 = \frac{n\sum tY - \sum t \sum Y}{n\sum t^2 - (\sum t)^2} \quad (13)$$

where b_1 is the slope of trend line; *Y* is *F*, *t* is time label; *n* is the sequence number of the monitoring year; $b_1 > 0$ and $b_1 < 0$ indicate that *F* has an increasing or decreasing tendency, respectively.

2.3.3. Quantitative analysis of the effects of different drivers

In this study, temperature (temp), precipitation (prec), sunshine duration (sun), average wind speed (wind), urbanization rate (urban), crop area (crop), livestock stocking rates (stock), and afforestation area (forest) were selected as the indicators used to assess the relationship among climate change and human activities. In detail, livestock stocking rates was expressed in sheep units. Large animals mainly included cows, horses, and donkeys, etc., where one of large animal equals five sheep units. On this basis, a multiple linear regression model was established to quantitative analysis the effects of climate change and human activities using Formula (14);

$$Y = a + b_1x_1 + b_2x_2 + b_3x_3 + \ldots + b_8x_8 \quad (14)$$

where *Y* is dependent variable, that is, *F*; x_1, x_2,… x_8 are independent variables; b_1, b_2,… b_8 are regression coefficients; *a* is the equation intercept.

3. Results

3.1. The dynamics of the soil retention rate in Inner Mongolia from 1981 to 2010

The average *F* increased gradually across the landscape from Southwestern to Northeastern Inner Mongolia in the early 1980s (1981–1983) and the end of the 2000s (2008–2010) (Fig. 2). Overall, the average of *F* did not change significantly over that time period, and only decreased insignificantly from 0.60 to 0.58. Over the past 30 years, the size of the area with $F < 0.2$ increased from 113,024 km^2 to 116,800 km^2; this occurred mainly in Western Inner Mongolia. Meanwhile, the area of with $F > 0.8$ decreased from 236,096 km^2 to 34,944 km^2; this occurred mainly in Northeastern Inner Mongolia, such as counties 25, 26, 55, and 84, etc.

Based on the trend analysis and Student's t test, the *F* experienced a decline from 1981 to 2010, with the total area experiencing a decrease covering 696,832 km^2. A significant decrease occurred within 382,400 km^2, including 54.88% of total area with a decrease in *F*; this mainly occurred in 59 counties, such as county 23 of Western Inner Mongolia, counties 10 and 59 of Central Inner Mongolia, and counties 16, 25, and 55 of Eastern Inner Mongolia, etc. Meanwhile, the total area with an increasing trend of *F* covered 424,064 km^2, of which 181,184 km^2 experienced a significant increase area, which accounted for 42.73% of total area with an increase. These regions were mainly distributed in counties 2, 3, and 57 of Western Inner Mongolia, counties 1, 61, and 62 of Central Inner Mongolia, etc., within a total of 18 counties. In addition, the area with a significantly increasing trend covered 457,920 km^2 from 2003 to 2010, accounting for 70.22% of the area with a significant change (Fig. 2d). Except for some counties in Eastern Inner Mongolia, such as counties 5, 6, 7, 8, 17, 25, 26, 55, 85, etc., the *F* experienced an significantly increasing trend in other regions. This was mainly attributed to the implementation of ecological engineering.

3.2. Quantitative identification of the drivers of a significant increase in the soil retention rate in various regions

The spatial distribution of the regions with a significant increase of *F* induced by different factors is shown in Fig. 3. In these regions, 124,096 km^2 were affected by climate change, accounting for 68.49% of the area with a significant increase of *F*. Temperature and wind speed were the major climatic factors. Specifically, the area with a significant increase of *F* induced by temperature, wind speed, and the coupled effects of these two factors totaled 98,624 km^2, which mainly occurred in counties 2 and 3 of Western Inner Mongolia, counties 1 and 61 of Central Inner Mongolia, and county 44 of Eastern Inner Mongolia. However, the spatial distribution of regions where significant changes in *F* were induced by the two climatic drivers varied when they were restricted by regional vegetation and soil heterogeneity. For example, the Badain Jaran Desert covered county 3 almost completely, and a decrease of wind was the main factor causing a significant change in *F*. In contrast, the *F* of Central and Eastern Inner Mongolia was more sensitive to temperature due to the relatively abundant vegetation, such as in county 61. Meanwhile, the effect of precipitation on *F* was mainly concentrated in county 62 of Central Inner Mongolia. In addition, 5440 km^2 was affected by the coupled effects of temperature, wind speed, and precipitation. Compared with other climate factors, the contribution of sunshine duration can be ignored.

Human activities cause a significant increase of *F* affected of 110,976 km^2, accounting for 61.25% of the area with a significant increase. Afforestation had the greatest influence on the change of *F*, and affected 41,152 km^2; this mainly occurred in counties 1, 61, and 62 of Central Inner Mongolia; the increase in vegetation cover in these regions had weakened the intensity of the wind and its sediment carrying capacity. Crop area was the second-most important human factor causing an increase of *F* in regions that mainly occurred in counties 2 and 24 of Western Inner Mongolia and county 44 of Eastern Inner Mongolia; here this change was mainly attributed to wasteland reclamation. The urbanization rate mainly affected the increase of *F* in county 3 of Western Inner Mongolia and county 64 of Central Inner Mongolia. Finding areas where the change of *F* was influenced by both climate change and human activities was not difficult in most counties; these areas were mainly concentrated in five regions (I1–I5) and 11 counties (Fig. 3). The area that affected by the coupled effect of climate change and human activities covered 110,016 km^2, which together explained 60.72% of the significant increase of *F*. Among them, the coupled effect of climatic factors and afforestation, and climatic factors and crop area had a strong effect on areas where the *F* increased. The former and the latter accounted for 22.71% and 22.01% of the

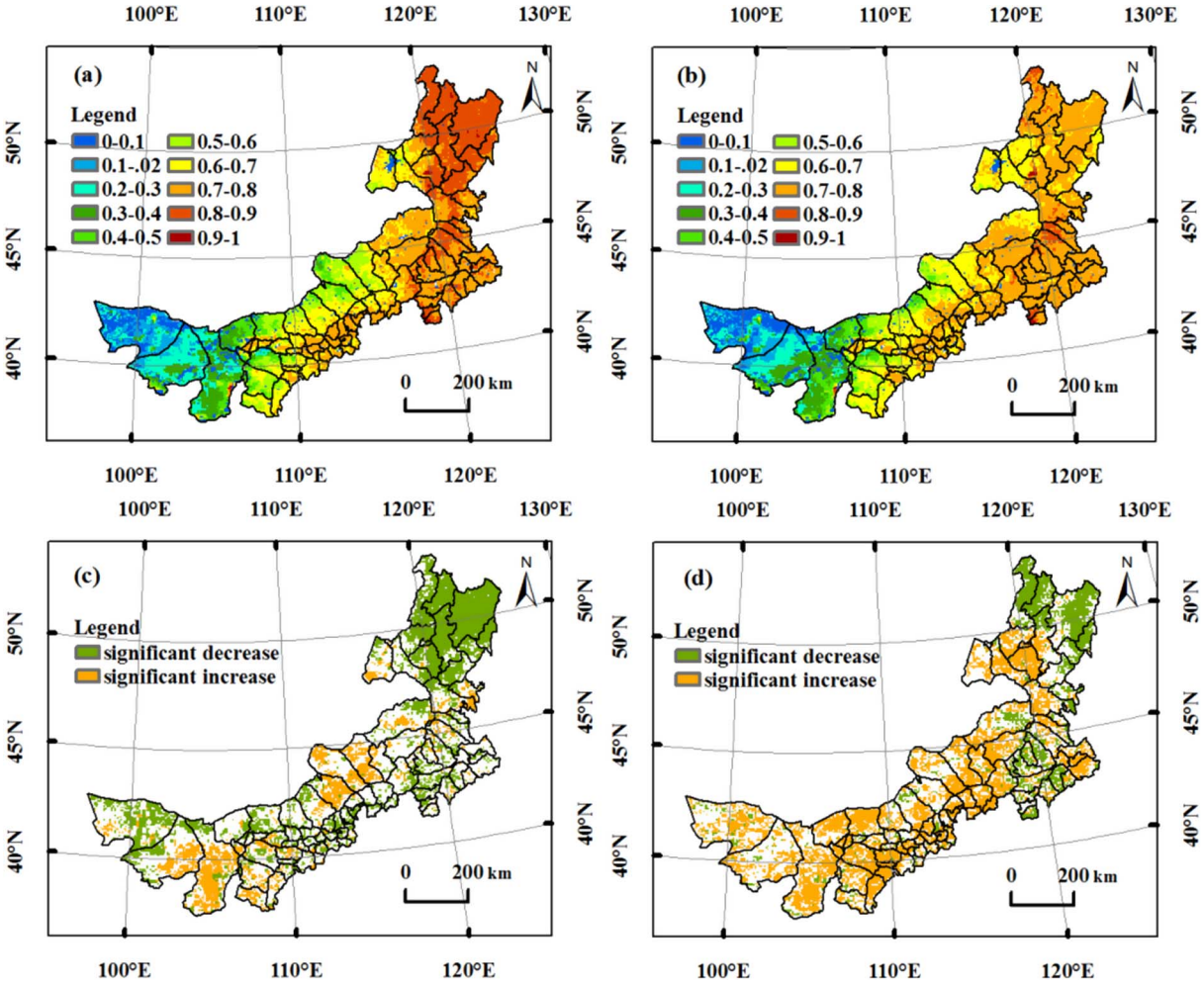

Fig. 2. Spatial distribution of the soil retention rate and its change during 1981–2010 years.

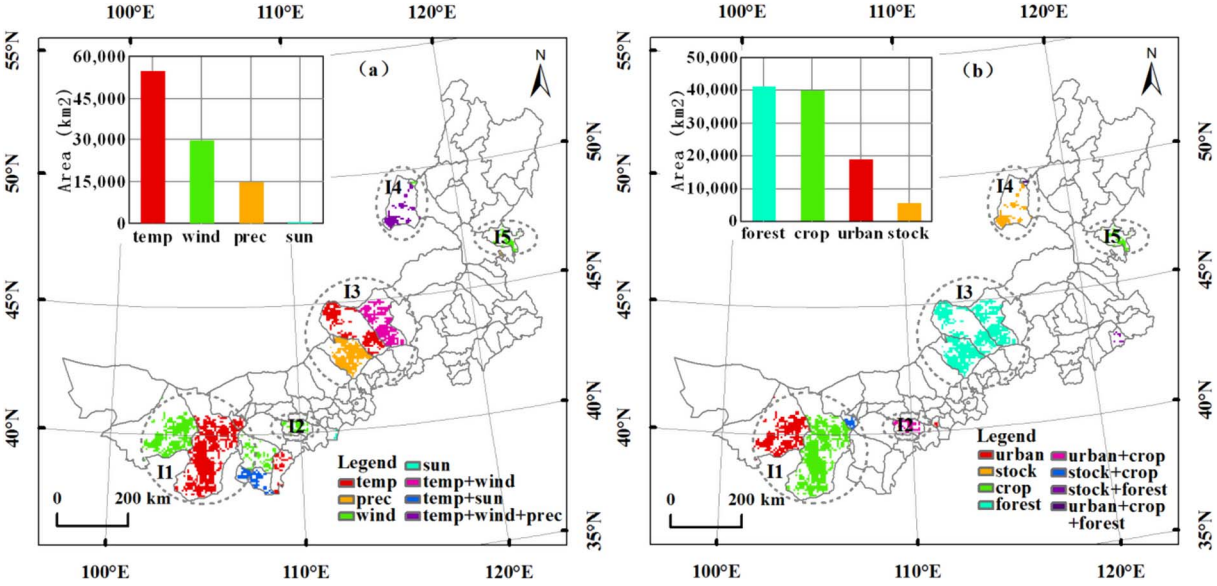

Fig. 3. Spatial distribution of climatic factors (a) and human activities (b) in the regions with a significant increase of soil retention rate.

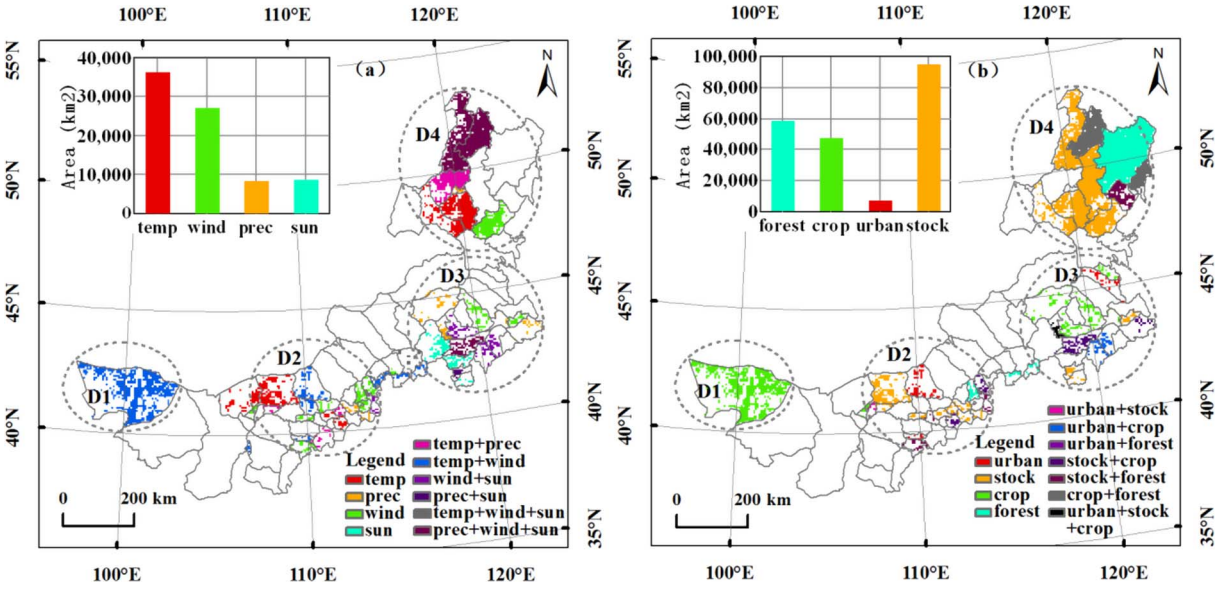

Fig. 4. Spatial distribution of climatic factors (a) and human activities (b) in the regions with a significant decrease of soil retention rate.

significant increase area, respectively, and were concentrated in the I3 region and in I1 and I5 regions, respectively.

3.3. Quantitative identification of the drivers of a significant decrease in the soil retention rate in various regions

The spatial distribution of the regions with a significant decrease of *F* induced by different factors is shown in Fig. 4. An area of 198,336 km^2 that was affected by climate change with a decrease in *F* accounted for 51.87% of the area with a significant decrease in *F*. The coupled effect of temperature and wind speed was the main driver that induced the decrease of *F*; high winds and strong evaporation had accelerated land degradation in county 23 of Western Inner Mongolia, counties 20 and 63 of Central Inner Mongolia, while 46,976 km^2 were influenced by the coupled effect of the two. Meanwhile, the areas with a significant decrease of *F* caused by the coupled effects of precipitation, wind speed, and sunshine duration covered 44,416 km^2. This mainly occurred in Eastern Inner Mongolia, such as counties 25, 26, and 54; in these regions, a decrease in precipitation rates combined with an increase in wind speed exacerbated the possibility of vegetation degradation and sandstorm hazards. In addition, temperature, as a single climatic factor, influenced an area of 36,288 km^2; this mainly occurred in counties 27 and 73 of Eastern and Western Inner Mongolia, respectively, with the rapid rise in temperature resulting in a decrease of *F* in these regions. Sunshine duration had a relatively small effect, which may be better reflected by its coupling with other driving factors.

Human activities caused a significant decrease of *F* over 261,440 km^2, accounting for 68.37% of the area with a significant decrease of *F* with livestock stocking rates serving as the dominant human factor. Livestock stocking rates caused a decrease of *F* over 94,784 km^2, which mainly occurred in counties 26, 27, 84, and 85 of Eastern Inner Mongolia and county 72 of Western Inner Mongolia. Overgrazing and less supervision of herds were the main causes that led to the decrease of *F*. Afforestation had a significant negative correlation with *F* in county 55 of Eastern Inner Mongolia and county 10 of Central Inner Mongolia; the area of these regions reached to 58,688 km^2, which might be attributed to damage to natural forests. The crop area and urbanization rate also had some effects on *F*, and the areas affected by the former and the latter covered 47,616 km^2 and 7296 km^2, respectively. In addition, 36 counties experienced a coupled effect of climate change and human activities, which were mainly concentrated in four regions (D1–D5; Fig. 4). The area influenced by these coupled effects covered 163,072 km^2, which together explained 42.64% of the significant decrease of *F*. The coupled effect of crop area and climatic factors as well as those of the coupled effects of livestock stocking rates and climatic factors were the main driving factors of this decreased *F*. In addition, the former was mainly concentrated in regions D1 and D3, while the latter was mainly concentrated in regions D2 and D4.

4. Discussion

Sandstorms cause damage and seriously affect the region of Inner Mongolia in China; many researchers have concluded that the driving factors of sand-stabilization services were relatively complex and influenced by both climate change and human activities (Du et al., 2016; Jiang et al., 2016a; Marquer et al., 2017). To investigate the driving forces of sand-stabilization services, a comprehensive and quantitative study was needed that integrated multiple factors. With respect to climatic drivers, our result showed that temperature played a significant role in the changes of *F*, which was consistent with the finding of Garbrecht et al. (2015) and Correa et al. (2016). The average temperature in Inner Mongolia increased from 4.18 °C in the 1980s to 5.17 °C in the 2010s, with a mean slope of 0.05 (Fig. 5a), which led to an increase of evaporation and strongly limited vegetation growth, especially for the growth of shrubs and sparse vegetation (Jiang et al., 2017). The coupled effects of warming, a tendency toward a drying climate, and unsustainable human activities further amplified the effects on the decrease of *F*; for example, previous studies had predicted that as temperatures increased by 2 °C wind erosion in grassland would increase by about 25% (Gao et al., 2002).

Under the background of overall warming in the region analyzed here, the influence of regional precipitation on the change of *F* would be further enhanced (de Beurs et al., 2015; Yu and Li, 2015). The change of precipitation varied significantly between the eastern and western parts of Inner Mongolia (Fig. 5c). Although precipitation had an insignificant effect on *F* in western regions, the increasing trend of precipitation and the improvement of hydrothermal conditions played positive role in reducing wind erosion in the desert (Tian et al., 2015), and led to an increase of *F* in counties 2 and 3. In eastern Inner Mongolia, the decrease in precipitation rates resulted in increased levels of stress on soil water, which was not conducive to vegetation growth (Yao et al., 2013). In the present study, we found *F* exhibited relatively high positive correlations with wind speed. During the past three decades, the average wind speed of Inner Mongolia decreased from 3.06 m/s in

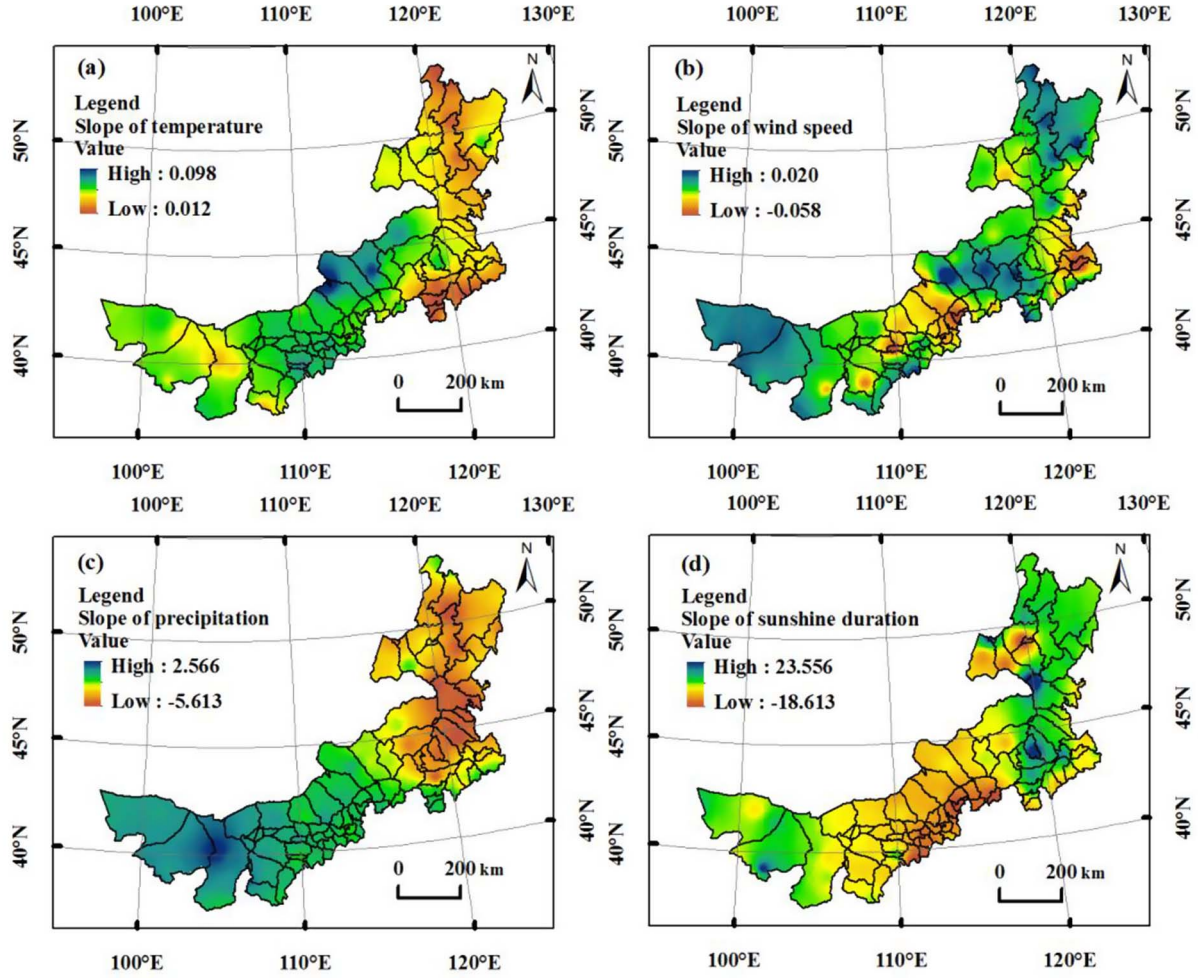

Fig. 5. Slope of annual temperature (a), wind speed (b), precipitation (c) and sunshine duration (d) in Inner Mongolia from 1981 to 2010.

the 1980s to 2.74 m/s in the 2010s, with a mean slope of −0.025 (Fig. 5b), which provided a favorable conditions for vegetation restoration and an increase of *F*. However, it was worth noting that the wind speed of some counties increased significantly during 2000–2010 and resulted a decrease of *F*; this indicated that wind speed was a main factor affecting the sandstorm activity in arid and semi-arid regions while our results also coincided with previous studies (Liu et al., 2015). Sunshine duration only contributed 0.31% and 4.29%, respectively, to the areas with a significant increase and decrease of *F*, and the effect may be better reflected by changes in temperature.

With the continuous improvement in the ability of human society to manage and control natural ecosystems, the effects of human activities on the change of *F* varied greatly. From 1981 to 2010, the protection and degradation of the ecosystem of Inner Mongolia almost happened simultaneously. The results here indicated that areas of afforestation had a marked impact on sand-stabilization services, especially in the areas where *F* increased significantly. During the past three decades, especially since 2002, the Beijing–Tianjin sandstorm source control project had compensated for the adverse effects of other human activities, and promoted an increase in *F* to some extent, which was more evident during 2003–2010 (Fig. 2d); this result was also in agreement with previous studies (Yang et al., 2015; Wu et al., 2016). However, ecological restoration projects should fully consider regional resource endowments and the carrying capacity of the environment; efforts to conduct afforestation may often backfire when these factors are not carefully considered. For example, Cao et al. (2007) found that large-scale afforestation on loess soils that would not naturally support a forest was likely to lead to an excessive consumption of soil moisture, and ultimately increase the risk of desertification and economic losses. The studies of Lu et al. (2016) and Zhang et al. (2016) reached similar conclusions. This also partly explained why afforestation has led to a decrease in *F* in counties 10 and 55.

In some counties, an increase of crop area had led to an increase of *F*, which was mainly caused by the conversion of unused land. For example, based on the analysis of the land use transfer matrix, 428 km^2 of unused land was converted to cultivated land in county 2 from 1981 to 2010. Excluding this situation, the results obtained here showed that farmland reclamation in counties 5, 8, 23, 74, 69, etc. that resulted in a decrease of *F* could be attributed to the exposure of the land surface and the exacerbation of wind erosion in dry conditions (Soranno et al., 1996; Zampella et al., 2007; Li et al., 2008). Rapid development of the animal husbandry industry has resulted in a significant increase in livestock stocking rates in Inner Mongolia in the past 30 years; excessive grazing coupled with farmland reclamation has resulted in a decrease in *F* (Fig. 6). However, the increase of livestock stocking rates did not aggravate grassland degradation in some regions, such as county 82, which was mainly attributed to the implementation of a grazing prohibition policy (Gu and Li, 2013). With the acceleration of urbanization, a large number of rural people had left the area to find new job opportunities in cities so that humans put less pressure on the land; this served as an important factor that led to vegetation recovery and an increase of *F* (Li et al., 2016), such as in counties 3, 64, etc. In contrast, rapid urbanization caused an increase in the construction of infrastructure and exploitation of energy; for example, total energy production increased from 1.08×10^7 to 4.97×10^8 tons of Standard Coal Equivalent in 1981–2010 years (Inner Mongolia Bureau of Statistics,

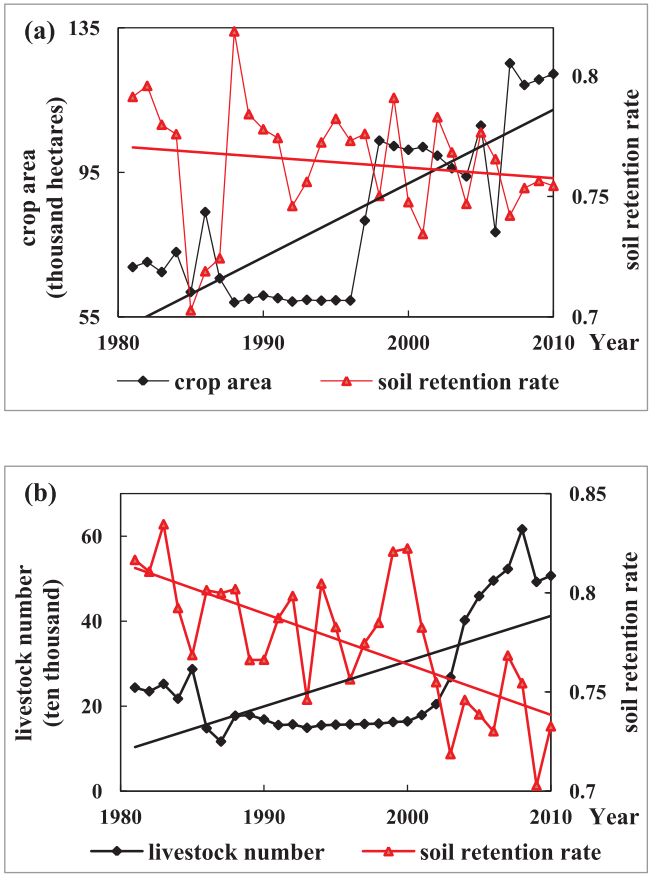

Fig. 6. Changes of crop area in county 5 (a) and livestock number in county 84 (b) from 1981 to 2010.

2011). Large-scale energy exploitation not only resulted in land surface subsidence and damage to plant roots, but also caused a falling groundwater and land degradation (Fan et al., 2015), which finally seriously affected sand-stabilization services.

Although the relative roles of different climatic and human factors on sand-stabilization services could be identified in this study, some uncertainties remained. First, the RWEQ model was originally developed based on American farmland. When combined with the natural environment in Inner Mongolia, cubic spline interpolation was used to convert soil particle content data. However, the converted soil particle content did not conform entirely to the range of parameters required by RWEQ model, which might lead to some deviations in the results. Second, linear regression analysis was carried out at county level by using the average value of factors as independent variables, which could not reflect the spatial differences within a single county. In the future, the social-economic data could be transferred to the grid data and a geographically weighted regression model (GWR) could be used to achieve a more detailed analysis. In addition, a non-parametric test method, such as the Mann–Kendall test, could be employed to avoid the uncertainties related to short-term extreme weather and mutation phenomenon (He et al., 2013). Finally, more independent variables, such as groundwater resources, road construction, per capita income of farmers and herdsmen, etc., and system dynamics models could be used to achieve a more comprehensive analysis of the effects of driving factors on sand-stabilization services in future studies.

5. Conclusion

From 1981 to 2010, the soil retention rate, *F*, in Inner Mongolia underwent a significant change driven by both climate change and human activities. Overall, *F* decreased in more areas than where *F* increased. A significant decrease was observed over 382,400 km^2, while a significant increase occurred over 181,184 km^2. With the implementation of Beijing–Tianjin sandstorm source control project, the area with a significant increase of *F* accounted for 70.22% of the area experiencing a significant change from 2003 to 2010, and the development of this project provided remarkable results.

Climate change and human activities had almost equivalent effects on the regions with a significant increase of *F*. Temperature, wind speed, and the coupled effect of the two were the main climate drivers, while afforestation and the coupling of afforestation with other factors were the main human drivers. The coupled effect of climate change and human activities also had a great impact on areas where the *F* increased, such as temperature and crop area, wind speed and urbanization rate, etc. In regions with a significant decrease of *F*, human activities played a more obvious role, which was mainly attributed to the increase of livestock stocking rates and crop area. In addition, crop area, livestock stocking rates and climatic factors were also the main coupled factors causing a significant decrease of *F*. During the period of 2003–2010, the implementation of a series of engineering measures had played an important role in improving the sand-stabilization service in Inner Mongolia, and also pointed out the logical direction for future environmental restoration of this ecologically fragile area. During future efforts to protect the ecosystem of this region, it will be crucial to protect and manage forest and grass vegetation, restrain the expansion of desertification and to control land use methods. Meanwhile, reasonable afforestation should be conducted within the capacity of this ecosystem along with the rational use land resources, in a way that will promote harmony between human beings and nature.

Acknowledgements

This research is jointly supported by National Key Research and Development Program of China (2016YFC0501002), and National Natural Science Foundation of China (71573245).

References

Arnaud, F., Poulenard, J., Giguet-Covex, C., Wilhelm, B., Revillon, S., Jenny, J.P., Revel, M., Enters, D., Bajard, M., Fouinat, L., Doyen, E., Simonneau, A., Pignol, C., Chapron, E., Vanniere, B., Sabatier, P., 2016. Erosion under climate and human pressures: an alpine lake sediment perspective. Quat. Sci. Rev. 152, 1–18.

Becker, N., Segev, M., Bar, P., 2015. Stabilization of sand dunes: do ecological and public perceptions go hand in hand? Reclaiming Landscapes for a Sustainable Future Land Restoration. 10.1016/B978-0-12-801231-4.00011.

Borrelli, P., Ballabio, C., Panagos, P., Montanarella, L., 2014. Wind erosion susceptibility of European soils. Geoderma 232, 471–478.

Cao, S.X., Chen, L., Xu, C.G., Liu, Z., 2007. Impact of three soil types on afforestation in China's Loess Plateau: growth and survival of six tree species and their effects on soil properties. Landscape Urban Plan. 83, 208–217.

Cao, S.X., Zhang, J.Z., Chen, L., Zhao, T.Y., 2016. Ecosystem water imbalances created during ecological restoration by afforestation in China, and lessons for other developing countries. J. Environ. Manage. 183, 843–849.

Cerdan, O., Govers, G., Le Bissonnais, Y., Van Oost, K., Poesen, J., Saby, N., Gobin, A., Vacca, A., Quinton, J., Auerswald, K., Klik, A., Kwaad, F.J.P.M., Raclot, D., Ionita, I., Rejman, J., Rousseva, S., Muxart, T., Roxo, M.J., Dostal, T., 2010. Rates and spatial variations of soil erosion in Europe: a study based on erosion plot data. Geomorphology 122, 167–177.

Chan, K.M.A., Shaw, M.R., Cameron, D.R., Underwood, E.C., Daily, G.C., 2006. Conservation planning for ecosystem services. PLoS. Biol. 4, 2138–2152.

Chepil, W.S., 1962. A compact rotary sieve and the importance of dry sieving in physical soil analysis. Soil Sci. Soc. Am. J. 26, 4–6.

Correa, S.W., Mello, C.R., Chou, S.C., Curi, N., Norton, L.D., 2016. Soil erosion risk associated with climate change at Mantaro River basin, Peruvian Andes. Catena 147, 110–124.

Costanza, R., dArge, R., deGroot, R., Farber, S., Grasso, M., Hannon, B., Limburg, K., Naeem, S., ONeill, R.V., Paruelo, J., Raskin, R.G., Sutton, P., vandenBelt, M., 1997. The value of the world's ecosystem services and natural capital. Nature 387, 253–260.

Daily, G.C., 1997. Nature's Services: Societal Dependence on Natural Ecosystems. Island Press, Washington.

de Beurs, K.M., Henebry, G.M., Owsley, B.C., Sokolik, I., 2015. Using multiple remote sensing perspectives to identify and attribute land surface dynamics in Central Asia 2001–2013. Remote Sens. Environ. 170, 48–61.

de Oro, L.A., Colazo, J.C., Buschiazzo, D.E., 2016. RWEQ - wind erosion predictions for variable soil roughness conditions. Aeolian Res. 20, 139–146.

Du, H.Q., Dou, S.T., Deng, X.H., Xue, X., Wang, T., 2016. Assessment of wind and water erosion risk in the watershed of the Ningxia-Inner Mongolia Reach of the Yellow River, China. Ecol. Indic. 67, 117–131.
Fan, X.S., Gao, J.X., Tian, M.R., Zhang, W., 2015. Resources depletion & ecological damage cost accounting and analysis related to the coal mining in Inner Mongolia. Arid Land Resour. Environ. 29 (9), 39–44 (in Chinese).
Feng, Q., Ma, H., Jiang, X.M., Wang, X., Cao, S.X., 2015. What has caused desertification in China? Sci. Rep.-Uk 5, 15998.
Foley, J.A., DeFries, R., Asner, G.P., Barford, C., Bonan, G., Carpenter, S.R., Chapin, F.S., Coe, M.T., Daily, G.C., Gibbs, H.K., Helkowski, J.H., Holloway, T., Howard, E.A., Kucharik, C.J., Monfreda, C., Patz, J.A., Prentice, I.C., Ramankutty, N., Snyder, P.K., 2005. Global consequences of land use. Science 309, 570–574.
Fryrear, D.W., Saleh, A., Bilbro, J.D., 1998. A single event wind erosion model. T. Asae 41, 1369–1374.
Fryrear, D.W., Bilbro, J.D., Saleh, A., Schomberg, H., Stout, J.E., Zobeck, T.M., 2000. RWEQ: improved wind erosion technology. J. Soil Water Conserv. 55, 183–189.
Fu, Q., Li, B., Hou, Y., Bi, X., Zhang, X.S., 2017. Effects of land use and climate change on ecosystem services in Central Asia's arid regions: a case study in Altay Prefecture, China. Sci. Total Environ. 607, 633–646.
Galati, A., Crescimanno, M., Gristina, L., Keesstra, S., Novara, A., 2016. Actual provision as an alternative criterion to improve the efficiency of payments for ecosystem services for C sequestration in semiarid vineyards. Agric. Syst. 144, 58–64.
Gao, Q., Ci, L., Yu, M., 2002. Modeling wind and water erosion in northern China under climate and land use changes. J. Soil Water Conserv. 57, 46–55.
J.D., Garbrecht, Nearing, M.A., Steiner, J.L., Zhang, X.J., Nichols, M.H., 2015. Can conservation trump impacts of climate change on soil erosion? An assessment from winter wheat cropland in the Southern Great Plains of the United States. Weather Clim. Extremes 10 (A), 32–39.
Gong, G.L., Liu, J.Y., Shao, Q.Q., 2014a. Effects of vegetation coverage change on soil conservation service of typical steppe in Inner Mongolia. Geo-Inf. Sci. 16 (3), 426–434 (in Chinese).
Gong, G.L., Liu, J.Y., Shao, Q.Q., 2014b. Wind erosion in Xilingol League, Inner Mongolia since the 1990s using the Revised Wind Erosion Equation. Prog. Geo 33 (6), 825–834 (in Chinese).
Gu, C.Y., Li, W.J., 2013. Research on the “grazing ban” policy's effect to grassland quality: analysis on the scale of herdsman households. Acta Sci. Nat. Univ. Pekin. 49 (2), 288–296.
He, W., Bu, R.C., Xiong, Z.P., Hu, Y.M., 2013. Characteristics of temperature and precipitation in Northeastern China from 1961 to 2005. Acta Ecol. Sin. 33 (2), 519–531 (in Chinese).
He, W.Q., Zhao, C.X., Gao, W.S., Chen, Y.Q., Qin, H.L., Fan, X.R., 2005. Main affecting factors of soil wind erosion under different land use patterns-a case study in Wuchuan County, Inner Mongolia. Chin. J. Appl. Ecol. 16 (11), 2092–2096 (in Chinese).
Hostert, P., Kuemmerle, T., Prishchepov, A., Sieber, A., Lambin, E.F., Radeloff, V.C., 2011. Rapid land use change after socio-economic disturbances: the collapse of the Soviet Union versus Chernobyl. Environ. Res. Lett. 6, 67–81.
Inner Mongolia Bureau of Statistics, 2011. Inner Mongolia Statistical Yearbook. China Statistics Press, Beijing (In Chinese).
Iturri, L.A., Avecilla, F., Hevia, G.G., Buschiazzo, D.E., 2016. Comparing adjacent cultivated and “virgin” soils in wind erosion affected environments can lead to errors in measuring soil degradation. Geoderma 264, 42–53.
Jiang, C., Li, D.Q., Wang, D.W., Zhang, L.B., 2016a. Quantification and assessment of changes in ecosystem service in the Three-River Headwaters Region, China as a result of climate variability and land cover change. Ecol. Indic. 66, 199–211.
Jiang, C., Wang, F., Zhang, H.Y., Dong, X.L., 2016b. Quantifying changes in multiple ecosystem services during 2000–2012 on the Loess Plateau, China, as a result of climate variability and ecological restoration. Ecol. Eng. 97, 258–271.
Jiang, L., Xiao, Y., Rao, E.M., Wang, L.Y., Ouyang, Z.Y., 2016c. Effects of land use and cover change (LUCC) on ecosystem sand fixing service in Inner Mongolia. Acta Ecol. Sin. 36 (12), 3734–3747 (in Chinese).
Jiang, L.L., Jiapaer, G., Bao, A.M., Guo, H., Ndayisaba, F., 2017. Vegetation dynamics and responses to climate change and human activities in Central Asia. Sci. Total Environ. 599, 967–980.
Kerns, B.K., Powell, D.C., Mellmann-Brown, S., Carnwath, G., Kim, J.B., 2017. Effects of projected climate change on vegetation in the Blue Mountains ecoregion, USA. Climate Serv. http://dx.doi.org/10.1016/j.cliser.2017.07.002.
Kidron, G.J., Ying, W., Starinsky, A., Herzberg, M., 2017. Drought effect on biocrust resilience: high-speed winds result in crust burial and crust rupture and flaking. Sci. Total Environ. 579, 848–859.
Keesstra, S., Nunes, J., Novara, A., Finger, D., Avelar, D., Kalantari, Z., Cerdà, A., 2018. The superior effect of nature based solutions in land management for enhancing ecosystem services. Sci. Total Environ. 610, 997–1009.
Kroeger, T., Manalo, P., 2007. Economic Benefits Provided by Natural Lands: Case Study of California’s Mojave Desert. Defenders of Wildlife report. Washington. < http://www.defenders.org/publications/mojaveeconomics > .
Latocha, A., Szymanowski, M., Jeziorska, J., Stec, M., Roszczewska, M., 2016. Effects of land abandonment and climate change on soil erosion–an example from depopulated agricultural lands in the Sudetes Mts, SW Poland. Catena 145, 128–141.
Li, S.K., Lu, M., Wang, K.R., Wang, X., 2008. Soil erosion of the main ground surface types influences on formation of dust storm in South Xinjiang. Sci. Agric. Sin. 41 (10), 3158–3167 (in Chinese).
Li, S.J., Sun, Z.G., Tan, M.H., Li, X.B., 2016. Effects of rural–urban migration on vegetation greenness in fragile areas: a case study of Inner Mongolia in China. J. Geogr. Sci. 26, 313–324.
Liu, F., Hao, Y.G., Xin, Z.M., Chen, H.L., Xu, J., Zhao, Y.M., 2014. The surface aeolian-sand flow structure in the northeastern margin of the Ulanbuh Desert. J. Desert Res. 34 (5), 1200–1207 (in Chinese).
Liu, L.Y., Yang, Y.Y., Shi, P.J., Zhang, G.M., Qu, Z.Q., 2015. The role of maximum wind speed in sand-transporting events. Geomorphology 238, 177–186.
Lu, C.X., Zhao, T.Y., Shi, X.L., Cao, S.X., 2016. Ecological restoration by afforestation may increase groundwater depth and create potentially large ecological and water opportunity costs in arid and semiarid China. J. Clean. Prod 10.1016/j.jclepro.2016.03.046.
Marquer, L., Gaillard, M.-J., Sugita, S., Poska, A., Trondman, A.-K., Mazier, F., Nielsen, A.B., Fyfe, R.M., Jönsson, A.M., Smith, B., Kaplan, J.O., Alenius, T., Birks, H.J.B., Bjune, A.E., Christiansen, J., Dodson, J., Edwards, K.J., Giesecke, T., Herzschuh, U., Kangur, M., Koff, T., Latałowa, M., Lechterbeck, J., Olofsson, J., Seppä, H., 2017. Quantifying the effects of land use and climate on Holocene vegetation in Europe. Quaternary Sci. Rev. 171, 20–31.
Marzen, M., Iserloh, T., de Lima, J.L.M.P., Fister, W., Ries, J.B., 2017. Impact of severe rain storms on soil erosion: experimental evaluation of wind-driven rain and its implications for natural hazard management. Sci. Total Environ. 590, 502–513.
McFarlane, D., Stone, R., Martens, S., Thomas, J., Silberstein, R., Ali, R., Hodgson, G., 2012. Climate change impacts on water yields and demands in south-western Australia. J. Hydrol. 475, 488–498.
Mendez, M.J., Buschiazzo, D.E., 2015. Soil coverage evolution and wind erosion risk on summer crops under contrasting tillage systems. Aeolian Res. 16, 117–124.
Millennium Ecosystem Assessment (MA), 2005. Ecosystems and Human Well-Being: Synthesis. Island Press, Washington.
Mo, H.W., Ren, Z.Y., Wang, X., 2006. Study on the dynamic change of value of vegetation sand-fixing effect – a case study in the Yuyang Region. Arid Zone Res. 23 (1), 56–59 (in Chinese).
Nelson, E., Mendoza, G., Regetz, J., Polasky, S., Tallis, H., Cameron, D.R., Chan, K.M.A., Daily, G.C., Goldstein, J., Kareiva, P.M., Lonsdorf, E., Naidoo, R., Ricketts, T.H., Shaw, M.R., 2009. Modeling multiple ecosystem services, biodiversity conservation, commodity production, and tradeoffs at landscape scales. Front. Ecol. Environ. 7, 4–11.
Pi, H.W., Sharratt, B., Feng, G., Lei, J.Q., 2017. Evaluation of two empirical wind erosion models in arid and semiarid regions of China and the USA. Environ. Modell. Softw. 91, 28–46.
Pierre, C., Kergoat, L., Bergametti, G., Mougin, E., Baron, C., Toure, A.A., Rajot, J.L., Hiernaux, P., Marticorena, B., Delon, C., 2015. Modeling vegetation and wind erosion from a millet field and from a rangeland: two Sahelian case studies. Aeolian Res. 19, 97–111.
Richardson, R.B., 2005. The Economic Benefits of California Desert Wildlands: 10 Years Since the California Desert Protection Act of 1994. The Wilderness Society Working Paper.
Schirpke, U., Kohler, M., Leitinger, G., Fontana, V., Tasser, E., Tappeiner, U., 2017. Future impacts of changing land-use and climate on ecosystem services of mountain grassland and their resilience. Ecosyst. Serv. 26, 79–94.
Schmidt, J., Werner, M.V., Schindewolf, M., 2017. Wind effects on soil erosion by water – a sensitivity analysis using model simulations on catchment scale. Catena 148, 168–175.
Serpa, D., Nunes, J.P., Santos, J., Sampaio, E., Jacinto, R., Veiga, S., Lima, J.C., Moreira, M., Corte-Real, J., Keizer, J.J., Abrantes, N., 2015. Impacts of climate and land use changes on the hydrological and erosion processes of two contrasting Mediterranean catchments. Sci. Total Environ. 538, 64–77.
Sharratt, B.S., Tatarko, J., Abatzoglou, J.T., Fox, F.A., Huggins, D., 2015. Implications of climate change on wind erosion of agricultural lands in the Columbia plateau. Weather Clim. Extremes 10, 20–31.
Shen, L., Tian, M.R., Gao, J.X., Qian, J.P., 2016. Spatio-temporal change of sand-fixing function and its driving forces in desertification control ecological function area of Hunshandake, China. Chin. J. Appl. Ecol. 27 (1), 73–82 (in Chinese).
Soranno, P.A., Hubler, S.L., Carpenter, S.R., Lathrop, R.C., 1996. Phosphorus loads to surface waters: a simple model to account for spatial pattern of land use. Ecol. Appl. 6, 865–878.
Steltzer, H., Landry, C., Painter, T.H., Anderson, J., Ayres, E., 2009. Biological consequences of earlier snowmelt from desert dust deposition in alpine landscapes. Proc. Natl. Acad. Sci. U.S.A. 106, 11629–11634.
Taylor, N.T., Davis, K.M., Abad, H., McClung, M.R., Moran, M.D., 2017. Ecosystem services of the Big Bend region of the Chihuahuan Desert. Ecosyst. Serv. 27, 48–57.
The Economics of Ecosystems and Biodiversity (TEEB), 2010. Mainstreaming the economics of nature: a synthesis of the approach. Conclusions and Recommendations of TEEB. Progress Press, Malta.
Tian, H.J., Cao, C.X., Chen, W., Bao, S.N., Yang, B., Myneni, R.B., 2015. Response of vegetation activity dynamic to climatic change and ecological restoration programs in Inner Mongolia from 2000 to 2012. Ecol. Eng. 82, 276–289.
UNEP, 2006. Global Deserts Outlook. United Nations Environment Programme, Nairobi.
Van Pelt, R.S., Zobeck, T.M., Potter, K.N., Stout, J.E., Popham, T.W., 2004. Validation of the wind erosion stochastic simulator (WESS) and the revised wind erosion equation (RWEQ) for single events. Environ. Modell. Softw. 19, 191–198.
Vu, Q.M., Le, Q.B., Frossard, E., Vlek, P.L.G., 2014. Socio-economic and biophysical determinants of land degradation in Vietnam: an integrated causal analysis at the national level. Land Use Policy 36, 605–617.
Wolfe, S.A., Nickling, W.G., 1993. The protective role of sparse vegetation in wind erosion. Prog. Phys. Geog. 17, 50–68.
Wu, D., Gong, G.L., Shao, Q.Q., Cao, W., 2016. Ecological effects assessment of Beijing and Tianjin sandstorm source control project. J. Arid Land Resour. Environ. 30 (11), 117–123 (in Chinese).
Yang, X.C., Xu, B., Jin, Y.X., Qin, Z.H., Ma, H.L., Li, J.Y., Zhao, F., Chen, S., Zhu, X.H., 2015. Remote sensing monitoring of grassland vegetation growth in the Beijing-Tianjin sandstorm source project area from 2000 to 2010. Ecol. Indic. 51, 244–251.

Yao, S.X., Zhao, C.C., Zhang, T.H., Liu, X.P., 2013. Response of the soil water content of mobile dunes to precipitation patterns in Inner Mongolia, northern China. J. Arid Environ. 97, 92–98.

Yu, Z., Li, X.L., 2015. Recent trends in daily temperature extremes over northeastern China (1960–2011). Quatern. Int. 380, 35–48.

Zampella, R.A., Laidig, K.J., Lowe, R.L., 2007. Distribution of diatoms in relation to land use and pH in blackwater coastal plain streams. Environ. Manage. 39, 369–384.

Zhang, J.Z., Zhao, T.Y., Jiang, C.C., Cao, S.X., 2016. Opportunity cost of water allocation to afforestation rather than conservation of natural vegetation in China. Land Use Policy 50, 67–73.

Zobeck, T.M., 1991. Soil properties affecting wind erosion. J Soil Water. Conserv. 46, 112–118.